Compton scattering of two x-ray photons by an atom

Alexey N. Hopersky, Alexey M. Nadolinsky, and Sergey A. Novikov[*]

Chair of Mathematics, Rostov State University of Transport Communication, Rostov-on-Don 344038, Russia

The process of inelastic nonresonant two x-ray free-electron laser (XFEL) photon Compton scattering by a free atom is theoretically investigated. The object of the study is the He atom. We obtain the absolute values and the shape of the double differential scattering cross section. The quantum effect of creation of "hot" scattered photons with maximum energy $2\hbar\omega - I_{1s}$ is predicted ($\hbar\omega$ is the energy of the incident XFEL photon on the atom, and I_{1s} is the energy of the ionization threshold of an atomic $1s^2$ shell).

I. INTRODUCTION

The creation of the x-ray free-electron laser (XFEL) offers an opportunity to study the fundamental processes of nonlinear interaction of electromagnetic radiation with a many-electron system. Such processes include, in particular, inelastic nonresonant Compton scattering of two x-ray photons by an atom. The first theoretical study of this process was carried out by the authors [1–3] under the assumption of attosecond duration of the interaction between the incident and scattered photons and the excited and ionized free atoms of Be and Ne. Experimentally, the effect of two XFEL photon Compton scattering by a many-electron system was first observed in [4] for metallic Be.

In this paper, we lift the requirement of attosecond duration for the photon-electron interaction. The object of the investigation is taken to be the helium atom (He: nuclear charge is $Z = 2$; the configuration and the term of the ground state are $[0] = 1s^2[^1S_0]$). This choice is due to primarily two factors. First, the helium atom is the simplest element with filled shells. Second, the atom of He is quite accessible and widely used for high-precision experiments. For example, in early work [5] the spectral resolution of the experiment when measuring the Compton profile of the scattering of a 98-keV photon by a free He atom was 470 eV. However, in recent studies [6], the magnitude of the spectral resolution for the experiment measuring the differential cross section of inelastic scattering of a 9.89-keV photon by a free He atom was 70 meV.

II. THEORY

Let us consider the process of inelastic nonresonant two XFEL photon Compton scattering by an atom of He:

$$\omega + \omega + [0] \rightarrow X \rightarrow 1s\varepsilon l + \omega_C, \tag{1}$$

where ω (ω_C) is the angular frequency of the incident (scattered, Compton) photon, X are the intermediate (virtual) scattering states, ε is the energy of the Compton electron of the continuous spectrum, and the orbital quantum number is $l \in [1,\infty)$. In Eq. (1) and from here forward we use the atomic system of units: $m_e = e = \hbar = 1$, where m_e is the electron mass, e is the electron charge, and $\hbar$ is Planck's constant. In the second (with respect to the number of interaction

vertices) order of nonrelativistic quantum perturbation theory, four probability amplitudes of process (1) interfering among themselves are determined over the following states:

$$\begin{cases} X_1 = 1sxp + \omega \\ X_2 = 1sx(l \pm 1) \\ X_3 = 1sx(l \pm 1) + \omega + \omega_C \\ X_4 = 1sxp + \omega + \omega + \omega_C. \end{cases} \tag{2}$$

The structure of electron configuration of atomic states in Eq. (2) corresponds to the choice of dipole approximation ($1s \rightarrow xp, x(l \pm 1) \rightarrow \varepsilon l$) for the radiative transition operator. Justification for this approximation is given in Sec. II of the paper.

The analytical structure of the probability amplitude of process (1) through the state X_1 (2) takes the following form (in Dirac notation):

$$W_{ij} = \sum_{x>F} \frac{\langle i|\widehat{H}_1|x\rangle\langle x|\widehat{H}_2|j\rangle}{E_i - E_x + i\gamma_{1s}}, \tag{3}$$

$$\widehat{H}_1 = -\frac{1}{c}\sum_{n=1}^{N}(\widehat{p}_n \cdot \widehat{A}_n), \tag{4}$$

$$\widehat{H}_2 = \frac{1}{2c^2}\sum_{n=1}^{N}(\widehat{A}_n \cdot \widehat{A}_n). \tag{5}$$

Here the following are identified: $\sum_{x>F}$ is a symbol of summation (integration) over a complete set of states of $1s \rightarrow xp$ excitation (ionization) of the atom; F is the Fermi level (the set of quantum numbers of the valence shell of the ground state of the atom); initial wave functions ($|i\rangle = |0;\omega\omega\rangle$); intermediate ($|x\rangle = |1sxp;\omega\rangle$) and final ($|j\rangle = |1s\varepsilon l;\omega_C\rangle$) scattering states; E_i is total Hartree-Fock energy of the $|i\rangle$ state; $\gamma_{1s} = \Gamma_{1s}/2$, Γ_{1s} is the natural width of the $1s$-vacancy decay; $\widehat{H}_1$ ($\widehat{H}_2$) is the operator of the radiation (contact) transition [7]; c is the speed of light in vacuum; $\widehat{p}_n$ is the momentum operator of the nth atomic electron; $\widehat{A}_n \equiv \widehat{A}(0;\vec{r}_n)$ is the electromagnetic field operator in the second-quantization representation (at time $t = 0$); $\vec{r}_n$ is the radius vector of the nth atomic electron and N is the number of electrons in the atom.

The probability amplitude (3) in the Feynman diagram representation of nonrelativistic quantum many-body theory is given in Fig. 1(a). We show that it is the leading contributor in the states X (2). Let us assume $\Gamma_{1s} = 0$. This approximation is justified by the value of $\Gamma_{1s} \approx 10^{-7}$ eV, which we estimated through extrapolation of the theoretical data [8] for the He
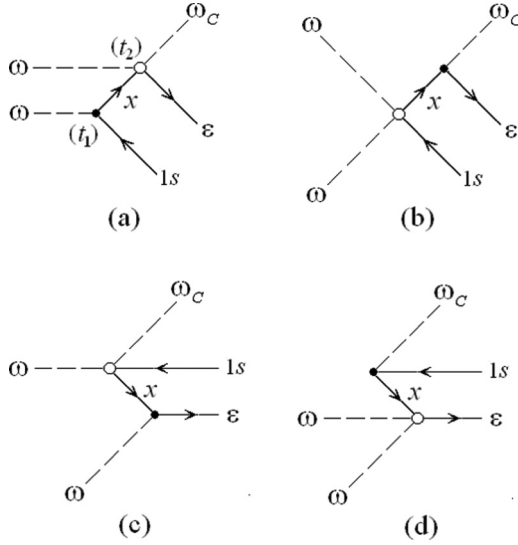
_____
[*]sanovikov@gmail.com

FIG. 1. Partial probability amplitudes for the inelastic nonresonant Compton scattering process of two XFEL photons by a He atom in the Feynman diagram representation. Arrow right, electron ($x \equiv xl'$, $\varepsilon \equiv \varepsilon l$); arrow left, vacancy ($1s$). Filled circle, interaction vertex via the radiative transition operator $\widehat{H}_1$; open circle, interaction vertex via the contact transition operator $\widehat{H}_2$. ω (ω_C) is the incident (scattered) photon. Time direction of the process is from left to right ($t_1 < t_2$). (a,b,c,d); see Sec. II of the paper.

atom. As a result, the energy denominator in Eq. (3) takes the form

$$(z + i\gamma_{1s})^{-1} \rightarrow \mathcal{P}\left(\frac{1}{z}\right) - i\pi\delta(z), \quad (6)$$

where $z = E_i - E_x$, symbol $\mathcal{P}$ denotes the Cauchy principal value of an integral, and δ is the Dirac delta function. Thus, in Eq. (3) we neglected the sum over the $|x\rangle$-discrete spectrum states due to $\gamma_{1s} = 0$ and the subsequent selection of incident XFEL photon energy $\omega \gg I_{1s}$. Here, $I_{1s} = 23.45$ eV is the energy of the ionization threshold of the $1s^2$ shell of the He atom (the calculation of this paper). In turn, due to $z \cong \omega - I_{1s} - x$, for $\omega \gg I_{1s}$ the singularity point at $x = \omega - I_{1s}$ is far from the value $x = 0$. This allows us to neglect the contribution from the Cauchy principal value of the integral in Eq. (3). Let us note here that theoretical investigation of the two-photon ionization of the hydrogen atom [9,10] showed the following. In the hard x-ray energy range of the absorbed photons, neglecting the Cauchy principal value of the integral for light atoms can lead to large errors in the absolute values of transition probability amplitudes. In the context of our work, this question requires further investigation. Now consider, for example, the probability amplitude of process (1) via the state X_2 (2). The structure of the amplitude in the Feynman diagram representation is given in Fig. 1(b). We take into account the theoretical result of work [11] for the probability amplitude of bremsstrahlung emission of a ω_C photon:

$$\langle 1sx(l \pm 1)|\widehat{H}_1|1s\varepsilon l; \omega_C \rangle \sim \delta(x - \varepsilon). \quad (7)$$

The exact analytical result for amplitude (7) with the continuum Hartree-Fock wave functions in the dipole approximation ($v/c \ll 1 \Rightarrow 2\omega \ll c^2 = 511$ keV, where v is the velocity

of the continuous spectrum electron) for operator (4) is given by formula (17) [11]. Along with the δ function, this formula includes the Cauchy principal value of the integral the contribution of which for $\omega_C \gg I_{1s}$ can be neglected. Note also the energy conservation for process (1):

$$\varepsilon \cong 2\omega - I_{1s} - \omega_C. \quad (8)$$

Under these approximations, the probability amplitude of the state X_2 (2) is proportional to $\delta(\omega_C) = 0$ for $\omega_C > 0$. Similarly, we find that the probability amplitude of the state X_3 (2) [Fig. 1(c)] is proportional to $\delta(\omega) = 0$ for $\omega > 0$. Finally, the integrand in the probability amplitude of the state X_4 (2) [Fig. 1(d)] is suppressed by the nonsingular energy denominator. Note that the Feynman diagrams of the third (three vertices of interaction operator $\widehat{H}_1$) and higher-order effects [due to Eq. (7)] can be discarded. Thus, in the following description of the differential cross section of the process (1) for $\Gamma_{1s} = 0$ and $\omega \gg I_{1s}$, it is sufficient to consider the probability amplitude of Eq. (3). At the same time, the following double inequality holds:

$$0 < \omega_C \leqslant \omega_C^{\max}, \quad (9)$$

where, according to Eq. (8), the cliff threshold energy of the Compton profile of the differential scattering cross section is defined to be $\omega_C^{\max} = 2\omega - I_{1s}$.

Consider the case of linearly polarized incident (parallel to each other) and scattered photons: $(\vec{e} \parallel \vec{e}_C) \perp P$. Here, $\vec{e}$ ($\vec{e}_C$) is the polarization vector of the incident (scattered) photon, and P is the scattering plane passing through the wave vectors of the incident ($\vec{k}$) and scattered ($\vec{k}_C$) photons. We write the triple-differential cross section of process (1) via the state X_1 (2) by following Fermi's golden rule:

$$d^3\sigma_{ij} = \frac{2\pi}{J}|W_{ij}|^2\delta(E_i - E_j)d^2f\, d\varepsilon. \quad (10)$$

Here, $J = cn/V$ is the density of flux of incident photons on the atom (in this case $n = 2$), V is the volume of quantization for the electromagnetic field, $d^2f = V(2\pi c)^{-3}\omega_C^2\, d\omega_C\, d\Omega$, and Ω is the spatial angle of emission of the scattered photon. At the same time, the radial part of the electron εl wave function is normalized over $\delta(\varepsilon - \varepsilon')$. Then, replacing the Dirac δ function by the Gauss instrumental spectral function (to account for the spectral resolution of the supposed experiment), integrating over the Compton electron energy (which is not recorded in the experiment), and summing over the intermediate and final scattering states (see Appendix A), from Eq. (10) we obtain for the double-differential cross section of process (1) via the state X_1 (2):

$$\frac{d^2\sigma_\perp}{d\omega_C\, d\Omega} \equiv \sigma_\perp^{(2)} = \eta\, r_0^2\, \beta\, \sigma_{1s} \int_0^\infty Q(x_0,\varepsilon)\, G(\varepsilon)\, d\varepsilon, \quad (11)$$

$$Q(x_0,\varepsilon) = \sum_{l=0}^\infty (l+1)\big[R_l^2(x_0 p;\varepsilon(l+1)) + \rho_l R_{l+1}^2(x_0 p;\varepsilon l)\big], \quad (12)$$

$$G(\varepsilon) = \frac{1}{\gamma_b\sqrt{\pi}}\exp\left[-\left(\frac{\varepsilon - \varepsilon_0}{\gamma_b}\right)^2\right]. \quad (13)$$

Here, the following quantities are defined: $\eta = 3\pi c/2$, r_0 is the classical electron radius, σ_{1s} is the photoionization cross section of the atomic $1s^2$ shell [12], $R_l(a,b) = \langle a|j_l(qr)|b\rangle$, $\rho_l = 0, l = 0; 1, l \geqslant 1$, j_l is the lth-order spherical Bessel function of the first kind, $q = |\vec{k} - \vec{k}_C| = (\omega/c)(1 + \beta^2 - 2\beta\cos\theta)^{1/2}$, $\beta = \omega_C/\omega$, θ is the scattering angle (the angle between wave vectors $\vec{k}$ and $\vec{k}_C$), $x_0 = \omega - I_{1s}$, $\varepsilon_0 = 2\omega - I_{1s} - \omega_C$, $\gamma_b = \Gamma_{\text{beam}}/(2\sqrt{\ln 2})$, and Γ_{beam} is the spectral resolution width of the scattered photon energy in the proposed experiment. In Eq. (11), it is taken into account that the statistical weight of the ground state of the He atom is equal to 1 ($S_0 = J_0 = 0$), and the quantization volume is taken as $V(cm^3) = c$ [13].

In concluding this section of the paper, we note two things. First, the calculation of the photoionization cross section in Eq. (11) was carried out by us in the dipole approximation for the $\widehat{H}_1$ operator. The condition of applicability of this approximation $\lambda \gg r_{1s}$ (λ is the wavelength of the incident photon; r_{1s} is the mean radius of the $1s^2$ shell) determines the boundaries for the studied energies of the incident photons from 500 eV ($\lambda = 24.810$ Å) to 1000 eV ($\lambda = 12.407$ Å). Then, $\lambda \gg r_{1s}(\text{He}) = 0.491$ Å. Second, both the photoionization cross section and the Q function were calculated in the single configuration Hartree-Fock approximation for transition wave functions. Accounting for the multipole, multiplicity, and many-body effects in describing the probability amplitudes $\langle i|\widehat{H}_1|x\rangle$ and $\langle x|\widehat{H}_2|j\rangle$ in Eq. (3) around the energy of the ionization threshold of the $1s^2$ shell is the subject of future research.

III. RESULTS AND DISCUSSION

The calculation results for the double-differential scattering cross section (11) are shown in Figs. 2 and 3.

The photoionization cross section is computed in the length form for the $\widehat{H}_1$ operator:

$$\sigma_{1s} = \tfrac{4}{3}\pi^2\alpha\, a_0^2\,\omega\,|M_{1s}|^2, \tag{14}$$

$$M_{1s} = \langle 1s_0|1s_+\rangle\langle 1s_0|\hat{r}|xp_+\rangle, \tag{15}$$

where α is the fine-structure constant, and a_0 is the Bohr radius. The radial part of the electron $1s_0$ wave function is obtained by solving the nonlinear integral-differential self-consistent-field Hartree-Fock equation for the configuration of the atomic ground state [0]. The radial parts of the electron $1s_+$ and xp_+ wave functions are obtained by solving the Hartree-Fock equations for $1s_+xp_+[^1P_1]$ configuration (taking into account the effect of radial relaxation [12] for ionization states of an atom in the field of the $1s$ vacancy). As expected (see the last paragraph of Sec. II), the result of our calculation $\sigma_{1s} = 1.864 \times 10^{-3}$ Mb is in good agreement with the theoretical result, for example [14], $\sigma_{1s} = 2 \times 10^{-3}$ Mb for $\omega = 600$ eV, whereas for $\omega = 100$ eV (the near-threshold region) our result $\sigma_{1s} = 0.304$ Mb is markedly different from the result of the experiment $\sigma_{1s} = 0.393$ Mb [15].

For a spherical Bessel function we used the Poisson integral representation [16],

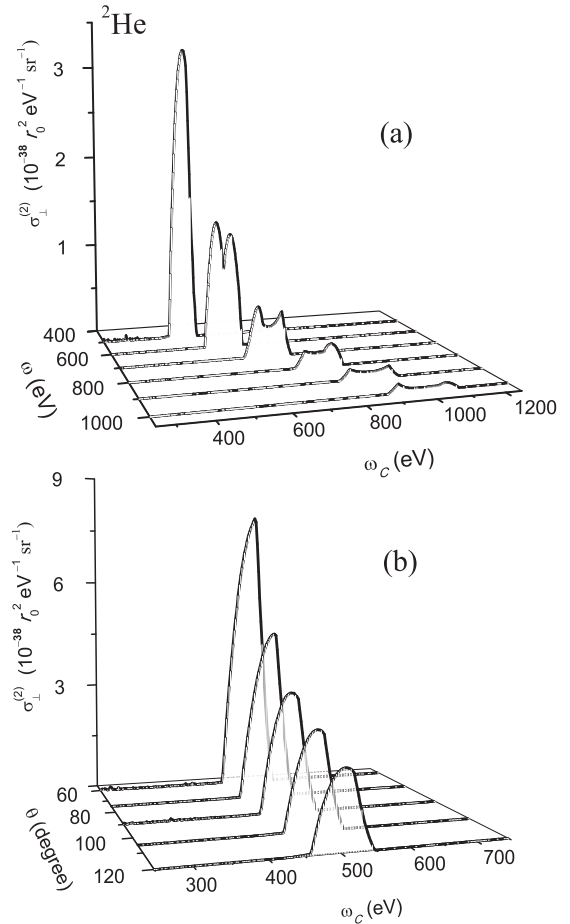$$j_l(x) = \frac{1}{l!}\left(\frac{x}{2}\right)^l \int_0^1 (1 - y^2)^l \cos{(xy)}\, dy, \tag{16}$$

FIG. 2. Double differential cross section for the inelastic nonresonant Compton scattering process of two linearly polarized (perpendicular to the scattering plane, $\perp$) XFEL photons by the He atom in the approximation $\Gamma_{1s} = 0$. (a) Dependence of the scattering cross section on the incident photon energy with $\theta = 90°$. (b) Angular distribution of scattered photons with $\omega = 500$ eV. $\Gamma_{\text{beam}} = 1.0$ eV, $I_{1s} = 23.45$ eV. $\omega\,(\omega_C)$ is the energy of the incident (scattered) photon, and θ is the scattering angle.

and the sum (12) accounts for multipolarity $l \in [0; 15]$. Accounting for values $l > 15$ is not more than 0.1% of the changes of absolute values of the double differential scattering cross section (11).

According to Fig. 2, the evolution of the double differential cross-section profiles before the Thomson scattering region (contact elastic scattering with $\omega_C = \omega$) qualitatively reproduces known results [17] for the normal (scattering of one photon by an atom) Compton scattering. Indeed, with the increase in both the incident photon energy [Fig. 2(a)] and the scattering angle [Fig. 2(b)], the maxima of Compton profiles become small and shift into the long-wave energy region of the ω_C photon. However, the appearance of the second incident photon not only quantitatively but also qualitatively changes the results of the generalized Compton scattering theory of $n(n \geqslant 1)$ photons by a free electron at rest. First of all, according to the generalized Compton
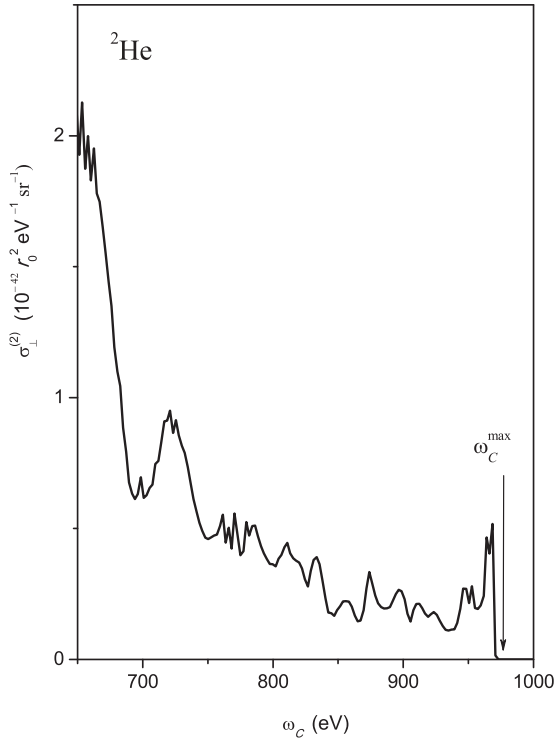
FIG. 3. Same as Fig. 2(a), but for $\omega_C \geqslant 650$ eV (the region of "hot" scattered photons). $\omega_C^{max} = 2\omega - I_{1s}$, $\omega = 500$ eV.

formula [18],

$$\omega_C = \frac{n\omega}{1 + (n\omega/\omega_0)(1 - \cos\theta)}, \quad (17)$$

$$\omega_0 = 2\pi c/\lambda_0, \quad \lambda_0 = 0.0243 \text{ Å}, \quad (18)$$

with, for example, $n = 1$, $\omega = 700$ eV, and $\theta = 90°$ the shift into the long-wave energy region of the ω_C photon should be equal to $\triangle\omega = \omega - \omega_C \cong 0.96$ eV, whereas according to Fig. 2(a) it is much larger, $\triangle\omega \cong 34$ eV. With $n = 2$, $\omega = 700$ eV, and $\theta = 90°$ Eq. (17) gives $\triangle\omega \cong 3.83$ eV $\ll 34$ eV. Second, an extended double differential cross-section structure appears after the Thomson scattering region, up to the region of "hot" ω_C-photon creation (Fig. 3). This structure has a clearly expressed oscillatory character as the Compton electron energy goes to zero: $\omega_C \rightarrow \omega_C^{max} \Rightarrow \varepsilon_0 \rightarrow 0$.

From comparison of results in Figs. 2 and 3, it follows that the probability to create a photon with energy $\omega_C \in (\omega - \triangle\omega; \omega + \triangle\omega)$ greatly exceeds the probability to create a hot photon. The nature of such drastic difference in the probability amplitude of creation is hidden in the mathematical structure of the Q function from Eq. (12). Indeed, this function is expressed via improper integrals of the first kind of the product of two wave functions of xp and εl electrons of the continuous spectrum. As a result (in the plane-wave approximation, see Appendix B), the criteria for the magnitude of these integrals are the values of the following parameter:

$$\zeta(\omega, \omega_C; \theta) = \frac{\sqrt{2}}{q}(\sqrt{x_0} - \sqrt{\varepsilon_0}). \quad (19)$$

Then, for energies ω_C satisfying the condition $\zeta \in (0; 1)$, we obtain the results in Fig. 2. With $\zeta > 1$ we obtain (for $\omega = 500$ eV) the double differential cross section for the creation of hot photons in Fig. 3. Already from Eq. (19) for $\varepsilon_0 \rightarrow 0$, it follows that $\zeta > 1$ for $x_0 \gg 0$. Thus, the appearance of high-energy electrons in the intermediate state leads to the effect of birth of hot photons. For that, of course, the wave function of a Compton electron with nearly zero energy should not be represented by a plane wave, but obtained as the solution of the Hartree-Fock equations with a vacancy in the $1s^2$ shell (Coulomb effects). In relation to this, an important question arises—of methodological investigation of the cross section for process (1) in the plane-wave approximation for electrons of the continuous spectrum and, thus, of determination of the role of Coulomb effects in the energy region $\approx \omega_C^{max}$. Solution to this problem may be obtained by the methods of Appendix B of this work, and is a subject of future investigations. Of course, if the XFEL radiation incident on the atom contains, for example, photons with energy $\omega_2 = 2\omega$ (the *second* harmonic of radiation), then the normal Compton scattering via channel $\omega_2 + [0] \rightarrow 1s\varepsilon l + \omega_C$ is a much more probable process. In this case, the same threshold for the Compton profile cliff is defined: $\omega_C^{max} = \omega_2 - I_{1s}$. This fact creates a problem of experimental "isolation" and observation of the quantum effects predicted in this paper. Nevertheless, the effect of hot ω_C-photon creation during inelastic nonresonant Compton scattering of two XFEL photons by a free atom may be very well accessible for experimental observation. The achieved and the expected brightness of the XFEL, and also results of many already performed experiments studying absorption processes of XFEL radiation by a free atom, also point to this possibility (see, for example, [19]). For example, when the number of photons in the x-ray pulse $N \cong 10^{31}$ (Feldhaus *et al.* [19]), the double-differential cross section for the creation of hot photons takes a quite measurable value of $\frac{N!}{2!(N-2)!}\sigma_\perp^{(2)} \approx 0.4 \times 10^{-5}$ (cm^2 eV^{-1} sr^{-1}).

IV. CONCLUSIONS

Nonrelativistic quantum theory for inelastic nonresonant two XFEL photon Compton scattering by free atoms is formulated. This process is considered as a quantum process implemented through the creation of a virtual state of excitation or ionization of an atom. As an example, the absolute values and the shape of the double differential scattering cross section for the atom of He are obtained. It is found that with the most probability Compton scattering of two x-ray photons by an atom is accompanied by the loss ($2\omega \rightarrow \omega_C \in (\omega - \triangle\omega; \omega + \triangle\omega), \triangle\omega \ll \omega$) of intensity of the incident XFEL radiation. It is shown that physical characteristics of the studied process differ significantly from those for the process of n-photon ($n \geqslant 1$) Compton scattering by a free resting electron. The main theoretical result is the effect of creation of hot scattered photons, with the maximum energy predicted to be $\omega_C^{max} = 2\omega - I_{1s}$. The question of an experimental observation of this effect for the case of a free atom continues to be open. Of course, an experimental observation of the predicted results (shown in Figs. 2 and 3) will provide further insight into such fundamental mathematical structures of the quantum multiphoton scattering theory as transition operators

(4) and (5), and also into the applicability of nonrelativistic quantum perturbation theory.

A generalization of the theory of this work for atoms with a nuclear charge $Z \geqslant 3$ is associated with taking into account new types of states of the virtual excitation or ionization of the atom. As a result, we should expect the appearance of new anomalous structures of the double differential scattering cross section due to intershell transitions in the atomic core. At the same time, heavy atoms ($Z \geqslant 20$) with drastically expressed resonance structure of the photoabsorption spectra of deep shells may present a special interest, for example, the $1s$-photoabsorption spectra of Cu ($Z = 29$) and Zn ($Z = 30$) atoms.

APPENDIX A

Let us state the analytical structure of the expression:

$$\sum_j \to \sum_T \sum_{MM'} |\langle {}^1P_1|\hat{L}|MT\rangle|^2, \qquad (A1)$$

$$\hat{L} = \sum_{n=1}^N \exp[i(\vec{q} \cdot \vec{r}_n)]. \qquad (A2)$$

Here (after expressing the photon part via creation and annihilation operators in the structure of $\widehat{H}_2$) are defined the electron parts of full wave functions of transition states $|{}^1P_1\rangle \equiv |1s x_0 p; {}^1P_1(J' = 1; M' = -1,0,1)\rangle$; $|MT\rangle \equiv |1s\varepsilon l; MT\rangle$; $T = LSJ$ is a term; and M is a projection of total angular momentum J of the final scattering state. Let us consider the following mathematical facts [20].

(a) Expansion of the exponent into a double functional series over spherical harmonics,

$$\exp[i(\vec{q} \cdot \vec{r}_n)] = \sum_{t=0}^\infty i^t [t] j_t(qr_n) \sum_{p=-t}^t (-1)^p C_{-p}^{(t)}(\vec{e}_q) C_p^{(t)}(\vec{e}_n), \qquad (A3)$$

where $\vec{e}_q$ ($\vec{e}_n$) is the unit vector in the direction of $\vec{q}$ ($\vec{r}_n$), $r_n = |\vec{r}_n|$, and $[t] = 2t + 1$.

(b) The Wigner-Eckart theorem,

$$\langle MT|D_p^{(t)}|{}^1P_1\rangle = (-1)^{J-M} \begin{pmatrix} J & t & 1 \\ -M & p & M' \end{pmatrix} (T\|D^{(t)}\|{}^1P_1), \qquad (A4)$$

for the scattering operator matrix element over multipoleness p:

$$D_p^{(t)} = \sum_{n=1}^N C_p^{(t)}(\vec{e}_n) j_t(qr_n). \qquad (A5)$$

(c) The orthogonality condition of Wigner $3j$ symbols ($\delta_{tt'}$ is the Kronecker-Weierstrass symbol),

$$\sum_{MM'} \begin{pmatrix} J & t & 1 \\ -M & p & M' \end{pmatrix} \begin{pmatrix} J & t' & 1 \\ -M & p' & M' \end{pmatrix} = \frac{1}{[t]} \delta_{tt'} \delta_{pp'}. \qquad (A6)$$

(d) The spherical harmonics summation theorem,

$$\sum_{p=-t}^t |C_{-p}^{(t)}(\vec{e}_q)|^2 = 1. \qquad (A7)$$

Using Eq. (29.8) from [21] and the equality for the Wigner $6j$ symbol,

$$\begin{Bmatrix} 1 & 1 & 0 \\ a & b & c \end{Bmatrix} = (-1)^{a-c+1} \frac{\delta_{ab}}{\sqrt{3[b]}}, \qquad (A8)$$

for the reduced matrix element in Eq. (A4) we have

$$({}^1P_1\|D^{(t)}\|T) = (1\|C^{(t)}\|l) R_t(x_0 p; \varepsilon l). \qquad (A9)$$

Then for Eq. (A1) we have

$$\sum_j \to \sum_{t=0}^\infty [t] (1\|C^{(t)}\|l)^2 R_t^2(x_0 p; \varepsilon l). \qquad (A10)$$

Finally, taking into account the triad condition $|l - 1| \leqslant t \leqslant l + 1$ ($l + t + 1 = 2g$, where g is an integer), the representation for the reduced matrix element of the spherical harmonic (in the standard phase system),

$$(1\|C^{(t)}\|l) = (-1)^g \sqrt{3[l]} \begin{pmatrix} l & t & 1 \\ 0 & 0 & 0 \end{pmatrix}, \qquad (A11)$$

as well as the Landau-Yang theorem about spin conservation for a system of two photons [22] [the $1s\varepsilon s({}^1S_0)$ state of the atomic system is forbidden as the final scattering state in Eq. (1)] from Eq. (A10), we obtain function $Q(x_0, \varepsilon)$ from Eq. (12).

APPENDIX B

In the plane-wave approximation for the continuous spectrum wave functions,

$$|x\rangle \sim \sin(r\sqrt{2x}), \quad |\varepsilon\rangle \sim \sin(r\sqrt{2\varepsilon}), \qquad (B1)$$

the Q function from Eq. (12) is defined via converging improper integrals of the first kind:

$$J_m^\pm = \int_0^\infty j_m(qr) \cos(rb_\pm) \, dr, \qquad (B2)$$

where $m = l, l + 1$ and $b_\pm = \sqrt{2}(\sqrt{x} \pm \sqrt{\varepsilon})$. Consider, for example, integral J_l^-. We introduce a critical parameter [see Eq. (19) in Sec. III] $\zeta = b_-/q$. Then, converting the result from [23], we obtain

$$J_l^- \sim \frac{1}{(1-z)^\alpha} F\left(\alpha, \alpha; \frac{1}{2}; \frac{z}{z-1}\right), \quad \zeta \in (0;1), \quad (B3)$$

$$J_l^- \sim F\left(\alpha, \alpha + \frac{1}{2}; 2\alpha + \frac{1}{2}; \frac{1}{z}\right) \cos(\pi\alpha), \quad \zeta > 1, \quad (B4)$$

where $z = \zeta^2$, $\alpha = (l + 1)/2$, and $F(a,b;c;z) \equiv {}_2F_1(a,b;c;z)$ is the hypergeometric function [24].

According to Eq. (B4), with $\zeta > 1$, only the odd-order Bessel functions give nonzero contributions to the Q function: $\cos(\pi\alpha) = (-1)^{n+1}$ with $l = 2n + 1 \Rightarrow j_l = j_{2n+1}$, $n \geqslant 0$. Precisely this fact leads to a quick ($\zeta = 1$—a point of discontinuity of the first kind) and significant reduction in the Q-function value with $\zeta > 1$. Analogous conclusion is also true for integral J_{l+1}^-: $l = 2n \Rightarrow j_{l+1} = j_{2n+1}$.

[1] A. N. Hopersky, A. M. Nadolinsky, and S. A. Novikov, Phys. Rev. A **88**, 032704 (2013).

[2] A. N. Hopersky, A. M. Nadolinsky, S. A. Novikov, and V. A. Yavna, Phys. Rev. A **91**, 022708 (2015).

[3] A. N. Hopersky, A. M. Nadolinsky, R. V. Koneev, and V. A. Yavna, Opt. Spectrosc. **119**, 187 (2015).

[4] M. Fuchs *et al.*, Nature Physics **11**, 964 (2015).

[5] P. Eisenberger and W. A. Reed, Phys. Rev. A **5**, 2085 (1972).

[6] B. P. Xie, L. F. Zhu, K. Yang, B. Zhou, N. Hiraoka, Y. Q. Cai, Y. Yao, C. Q. Wu, E. L. Wang, and D. L. Feng, Phys. Rev. A **82**, 032501 (2010); L. F. Zhu, L. S. Wang, B. P. Xie, K. Yang, N. Hiraoka, Y. Q. Cai, and D. L. Feng, J. Phys. B **44**, 025203 (2011).

[7] P. A. M. Dirac, *The Principles of Quantum Mechanics* (Clarendon, Oxford, 1958).

[8] O. Keski-Rahkonen and M. O. Krause, At. Data Nucl. Data Tables **14**, 139 (1974).

[9] H. R. Varma, M. F. Ciappina, N. Rohringer, and R. Santra, Phys. Rev. A **80**, 053424 (2009).

[10] V. Florescu, O. Budriga, and H. Bachau, Phys. Rev. A **84**, 033425 (2011).

[11] S. A. Novikov and A. N. Hopersky, J. Phys. B **44**, 235001 (2011).

[12] M. Ya. Amusia, *Atomic Photoeffect* (Plenum, New York, 1990).

[13] N. Bloembergen, *Nonlinear Optics* (W. A. Benjamin, New York, 1965).

[14] J. J. Yeh and I. Lindau, At. Data Nucl. Data Tables **32**, 1 (1985).

[15] J. A. P. Samson and W. C. Stolte, J. Electron Spectrosc. Relat. Phenom. **123**, 265 (2002).

[16] H. Bateman and A. Erdélyi, *Higher Transcendental Functions* (McGraw-Hill, New York, 1953), Vol. 2.

[17] F. Biggs, L. B. Mendelsohn, and J. B. Mann, At. Data Nucl. Data Tables **16**, 201 (1975); M. Jung, R. W. Dunford, D. S. Gemmell, E. P. Kanter, B. Krässig, T. W. LeBrun, S. H. Southworth, L. Young, J. P. J. Carney, L. LaJohn, R. H. Pratt, and P. M. Bergstrom, Jr., Phys. Rev. Lett. **81**, 1596 (1998); P. Jaiswal and A. Shukla, Phys. Rev. A **75**, 022504 (2007); L. A. LaJohn, *ibid.* **81**, 043404 (2010).

[18] A. H. Compton, Phys. Rev. **21**, 483 (1923); L. S. Brown and T. W. B. Kibble, *ibid.* **133**, A705 (1964); A. I. Nikishov and V. I. Ritus, J. Exp. Theor. Phys. **19**, 529 (1964); I. I. Goldman, Phys. Lett. **8**, 103 (1964); F. Ehlotzky, K. Krajewska, and J. Z. Kaminski, Rep. Prog. Phys. **72**, 046401 (2009); A. Di Piazza, C. Müller, K. Z. Hatsagortsyan, and C. H. Keitel, Rev. Mod. Phys. **84**, 1177 (2012).

[19] L. Young *et al.*, Nature (London) **466**, 56 (2010); G. Doumy *et al.*, Phys. Rev. Lett. **106**, 083002 (2011); N. Rohringer *et al.*, Nature (London) **481**, 488 (2012); H. Fukuzawa *et al.*, Phys. Rev. Lett. **110**, 173005 (2013); J. Feldhaus *et al.*, J. Phys. B **46**, 164002 (2013); K. Tamasaku *et al.*, Nat. Photon. **8**, 313 (2014).

[20] R. Karazija, *Introduction to the Theory of X-Ray and Electronic Spectra of Free Atoms* (Plenum, New York, 1996).

[21] A. P. Jucys and A. J. Savukynas, *Mathematical Foundations of the Atomic Theory* (Mintis, Vilnius, 1973) [in Russian].

[22] L. D. Landau, Dokl. Akad. Nauk SSSR **60**, 207 (1948) [in Russian]; C. N. Yang, Phys. Rev. **77**, 242 (1950).

[23] A. P. Prudnikov, J. A. Brychkov, and O. I. Marichev, *Integrals and Series* (Gordon and Breach Science, Amsterdam, 1986), Vol. 2.

[24] *Handbook of Mathematical Functions*, Natl. Bur. Stand. Appl. Math. Ser. No. 55, edited by M. Abramowitz and I. A. Stegun (U.S. GPO, Washington, D.C., 1972).